Penetration of self-affine fractal rough rigid bodies into a model elastomer having a linear viscous rheology

Silvio Kürschner and Valentin L. Popov
Berlin University of Technology, 10623 Berlin, Germany
(Received 6 December 2012; published 2 April 2013)

The penetration of a rigid body with a randomly rough, self-affine surface in a half space filled with a linearly viscous elastomer is studied numerically using the method of boundary elements. Using Radok's principle of functional equations, it is shown analytically that this problem is closely related to the recently investigated problem of contact of self-affine surfaces with an elastic half space. We show that the penetration velocity occurs to be a power function of the applied force and time, the corresponding exponents depending only on the Hurst exponent. For comparison, the same problem is solved using the method of reduction of dimensionality. Both three-dimensional numerical results and the method of reduction of dimensionality support the analytical predictions provided by general scaling arguments.

DOI: 10.1103/PhysRevE.87.042802 PACS number(s): 81.40.Pq, 46.55.+d, 62.20.Qp, 73.40.Cg

I. INTRODUCTION

The dynamics of the penetration of a rigid body into a viscoelastic medium plays an important role in many technological processes such as lithography [1], adhesion of soft and biological tissues [2], and heat transfer in elastomer contacts [3] as well as elastomer friction [4]. In all these problems, the surface roughness plays a decisive role [5]. While the contact of *elastic bodies* with rough surfaces has been intensively studied in the past [6,7] and has become again a hot topic in the last few years [8–13], the three-dimensional contact of fractal rough surfaces with *elastomers* has not been studied yet by direct numeral simulations.

In the present paper, we consider a contact of a rigid rough body with a model elastomer having the simplest possible rheology—a linearly viscous medium. Using this simple rheology allows us to reduce the number of parameters to a minimum and get transparent results of general applicability. The use of the linear rheology is further justified by the fact that in the medium frequency range, in which the loss modulus of an elastomer is larger than its storage modulus, most elastomers behave like a purely linear fluid [14]. We wish to stress, however, that while the rheological properties of the considered medium are those of a linearly viscous fluid, the boundary conditions are completely different. Bearing in mind the applications to contact mechanics of elastomers, we use no-friction and no-adhesion boundary conditions and neglect any capillary effects. The results of this paper, therefore, cannot be applied to the penetration of real fluids.

A general procedure to construct solutions of contacts with viscoelastic bodies using the known solutions for elastic bodies was formulated in the 1950s by Lee and Radok [15,16] by suggesting the principle of functional equations. This initial approach was applicable for a monotonous penetration into a viscoelastic medium [17]. In [18,19], it has been generalized for the case of an arbitrary loading; however, this is at the cost of high complexity. Recently, this principle was extended [20] and applied to more general problems [21,22]. In the present paper we apply Radok's principle to the contact of randomly rough, fractal surfaces.

This paper pursues two aims: First, we numerically investigate the three-dimensional contact problem of a fractal rough surface with a linearly viscous elastomer. Secondly, the obtained results are compared with the findings of the method of reduction of dimensionality [13,23–25].

II. DIMENSIONAL ANALYSIS

Consider a rigid cylindrical indenter with the diameter L. The cylinder is now slowly indented into a half space filled with a linearly viscous incompressible elastomer (viscosity η) initially having a flat surface, so that the axis of the cylinder is normal to the nondisturbed surface of the elastomer. The surface of the indenter is assumed to have a fractal, self-affine roughness at all scales up to the size L of the indenter, and is described by the spectral density $C_{2D}(q) \propto q^{-2(H+1)}$, where q is the wave vector and H is the Hurst exponent ranging from 0 to 1 [26]. The indentation is induced by a constant normal force F. In the following, we assume that the slope of the elastomer surface remains small in any point; thus the standard "half space approximation" is applicable [14]. Because of the slowness of the indentation, the inertia effects are neglected [27].

The general form of the inter-relation between the force F, the indentation depth u, and indentation velocity v can be found by simple scaling and dimensional arguments. First note that the form of the contact area depends on the indentation depth u only, but not on the indentation history. It further does not change, if the indentation depth and the rms roughness h are both multiplied with the same factor. Thus, the configuration of the contact area can only be a function of the ratio u/h. For any given contact configuration, the normal force F is strictly proportional to the shear viscosity η of the fluid and to the current indentation velocity v. Thus, we come to the conclusion that the ratio $F/(\eta v)$ should be a function of the nondimensional variable u/h. The only possibility to make the variable $F/(\eta v)$ nondimensional too, is to divide it by L. Thus, the dependence we search for must have the following general form:

$$\frac{F}{\eta L v} = f_H\left(\frac{u}{h}\right), \tag{1}$$

where f_H is an arbitrary function, which can depend on the Hurst exponent. Writing $v = du/dt$, separating variables, and integrating the resulting equation leads to the following general inter-relation of the indentation velocity and time:

$$\frac{vt}{h} = \psi\left(\frac{Ft}{\eta h L}\right), \tag{2}$$

where $\psi(\cdots)$ is a new function, which is connected with $f_H(\cdots)$ in a complicated way, so that we do not specify this inter-relation here.

III. BOUNDARY ELEMENT SIMULATIONS

To check this scaling relation, indentations were simulated numerically. We applied the boundary element method with an iterative multilevel algorithm similar to those used in [12] for the contact of elastic bodies. Bearing in mind the application to elastomer contacts, boundary conditions were used which normally apply in the case of a nonadhesive nonfrictional normal contact of elastic solids (no penetration, no adhesion, and no friction). Using Radok's principle of functional equations [16], one can show that the Green's function of the viscous problem can be obtained by replacing the shear modulus by the shear viscosity and the normal displacement by the normal velocity. The main difference with the elastic problem is that the stresses in the viscous medium are determined by the indentation velocity, while the boundary conditions are formulated in terms of displacements. In the course of time, the indentation depth changes and, in general, the contact configuration changes as well. Hence, one must solve the contact problem in every single time step. The details of the algorithm are described in [28]. Simulations were made for 36 different combinations of normal force, viscosity, maximum cross section, rms roughness, and Hurst exponent. The indenters' surfaces were circular with a diameter of 257 elements (51 432 elements in total). Obviously, the number of elements is much smaller than usually used for current studies of elastic contact problems [9–13]. This is due to a significant difference between the elastic and the viscous problem. To describe the solution of the elastic problem (for any given set of parameters), one must solve it only once, because it is a time-independent state. On the other hand, to describe the viscous solution, one must solve it whenever the contact geometry changes, because it is a time-dependent process. Therefore, each indentation consists of some hundreds to millions of contact problems, depending on the number of elements and on the required accuracy.

Four different Hurst exponents ($H = 0.1, 0.4, 0.6, 0.9$) were studied. Figure 1 shows graphical representations of such

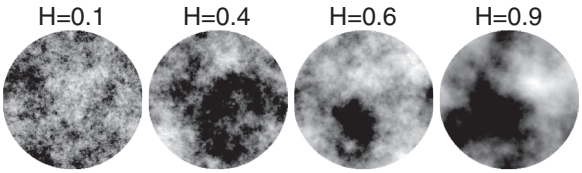

FIG. 1. Graphical representations of fractal indenter surfaces having different Hurst exponents. Darker colors denote higher peaks. Data have been scaled for optimal contrast in each picture.

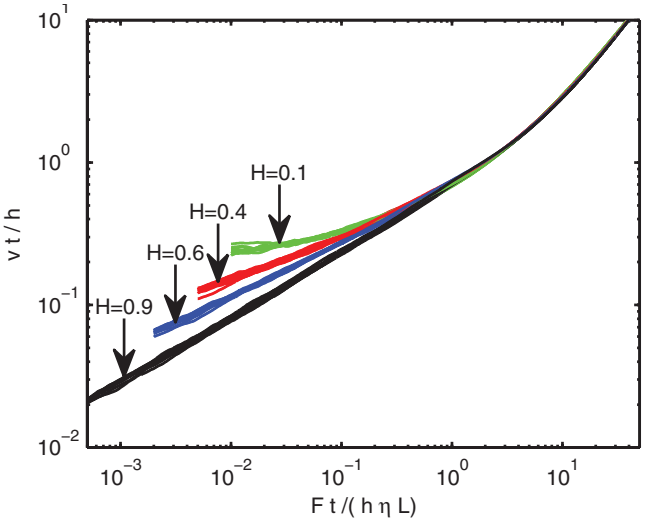

FIG. 2. (Color online) Plot of vt/h as a function of $Ft/(\eta h L)$ obtained by boundary element calculations. Each line represents the ensemble average over at least 80 indentations with identical parameters.

surfaces. The kinetics of the indentation represented in dimensionless variables vt/h and $Ft/(h\eta L)$, appearing in Eq. (2) is shown in Fig. 2. All curves were obtained by ensemble averaging over at least 80 randomly generated surface realizations with identical parameters. Curves with the same color correspond to identical Hurst exponents. For each Hurst exponent, nine different combinations of normal force, viscosity, diameter of the indenter, and rms roughness were used. All dependencies of indentation depth on time have three regions of qualitatively different behavior: (a) They start with a linear part with a universal slope 1. (b) The following second part is different for different Hurst exponents. (c) Finally, at large indentation depths, all curves collapse to one line with the slope 1. The physical sense of these three regions is very simple. The region (a) represents the time span when exactly one element of the indenter is in contact with the fluid and the body moves with a constant velocity. This part depends on finite size effects and thus is an artifact of the discretization. Therefore, this part is not shown in Fig. 2. In the region (b), the curves separate when the contact area starts to increase. This happens first for surfaces with high Hurst exponents. In all cases, where there are a few contact spots, all the dependencies in the region (b) are nearly linear in double logarithmic axes; thus a power law is applicable. Finally, the last region (c) corresponds to an almost complete contact. In the following, we concentrate our attention on the region (b) of small indentation depth, thus considering the initial stage of the indentation.

IV. THE ANALOGY TO THE NORMAL CONTACT PROBLEM OF ELASTICITY

One can easily see that the results for the same Hurst exponent always collapse to a single "master curve" thus supporting the functional form (2). The power law in the region (b) can be derived analytically from the results for an elastic contact of rough surfaces. In [12,13], Pohrt *et al.* derived the

power-law dependence of the incremental stiffness of an elastic contact with a randomly rough, self-affine surface with Hurst exponent H, which in the case of a noncompressive body has the form:

$$\frac{1}{4GL}\frac{\mathrm{d}F}{\mathrm{d}u} = \zeta\left(\frac{F}{4GhL}\right)^{\alpha}. \tag{3}$$

In [13], the following empirical approximation has been found for ζ:

$$\zeta \approx \frac{\pi(3-H)}{10}. \tag{4}$$

The power α has been shown to be described well by

$$\alpha = \frac{1}{1+H}, \tag{5}$$

at least for all Hurst exponents in the interval $H \in (0.4,1)$. For the limit $H \to 1$, this is an exact relation following from rigorous scaling considerations [13].

Separating variables in Eq. (3) and integrating over u with the initial condition $u(F=0)=0$ gives for $\alpha < 1$,

$$u = \frac{\zeta^{-1}h}{1-\alpha}\left(\frac{F}{4GLh}\right)^{1-\alpha}. \tag{6}$$

According to Radok [16], the Laplace transform is applied to Eq. (6). The external force is redefined as $F(t) = FH(t)$, with $H(t)$ being the Heaviside step function to meet the initial conditions. Within the Laplace domain the elastic properties are replaced by the viscous ones, meaning $G \mapsto \eta s$ [28]. One obtains

$$U(s) := [\mathcal{L}\{u\}(s)]_{G\mapsto\eta s} = \frac{\zeta^{-1}h}{1-\alpha}\left(\frac{F}{4\eta hL}\right)^{1-\alpha} s^{\alpha-2}. \tag{7}$$

This equation is transferred back to the time domain by application of the inverse Laplace transform, giving the indentation depths:

$$u(t) := \mathcal{L}^{-1}\{U(s)\} = \frac{\zeta^{-1}h}{(1-\alpha)\Gamma(2-\alpha)}\left(\frac{Ft}{4\eta hL}\right)^{1-\alpha}, \tag{8}$$

where Γ denotes the Gamma function $\Gamma(x) = \int_0^\infty t^{x-1}e^{-t}dt$. Rearranging this equation, differentiating with respect to time, and multiplying the result with t gives the following power law for dependence of the variable vt/h with respect to time:

$$\frac{vt}{h} = \frac{\zeta^{-1}}{\Gamma(2-\alpha)}\left(\frac{Ft}{4\eta hL}\right)^{\beta}, \tag{9}$$

with

$$\beta = 1-\alpha \approx \frac{H}{1+H}. \tag{10}$$

Our simulations confirm the power law (9). However, we have found that the numerical results can be better fitted with a somewhat different prefactor,

$$\zeta \approx 2-H, \tag{11}$$

instead of (4). With Eqs. (10) and (11), the power law (9) can be rewritten as

$$\frac{vt}{h} = \frac{1}{(2-H)\Gamma\left(\frac{1+2H}{1+H}\right)}\left(\frac{Ft}{4\eta hL}\right)^{\frac{H}{1+H}}. \tag{12}$$

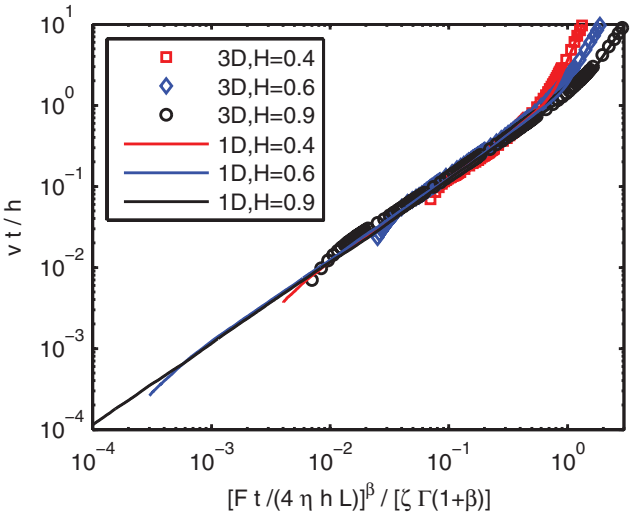

FIG. 3. (Color online) The dependency of the left side of Eq. (12) on its right side. Three-dimensional indentations are marked by symbols as described in the legend. For comparison, one-dimensional indentations with a much finer discretization are plotted with solid lines.

Figure 3 shows the dependence of its left side on its right side, both of them being dimensionless. In the region (b), all results collapse to a single "master curve," thus, confirming the analytical approximation (9).

V. METHOD OF REDUCTION OF DIMENSIONALITY

Let us analyze the same problem in the framework of the method of reduction of dimensionality. This method allows reducing a three-dimensional contact problem to a one-dimensional one; it was proposed in [29,30]. The validity of the method of reduction of dimensionality was proved with mathematical exactness for normal contact of arbitrary bodies of revolution in [24,25]. The method was shown to be applicable to normal contact of rough elastic solids [13]. In [28], it was extended to the case of dipping a rigid body into a linearly viscous elastomer and it was shown both analytically and by comparison with numerical simulations that the method of reduction of dimensionality can be used for viscous bodies too, as already argued in [14]. The present state of the method and its applications are presented in the review paper [31]. There has been public discussion about limits to the method of reduction of dimensionality when applied to contacts of random roughness. The main objection was that the one-dimensional substitute system has no inter-relations between elements of the elastic (or viscoelastic) foundation and, thus, cannot describe the original three-dimensional system having such correlations. Another objection was that for viscoelastic bodies, the elastic modulus is frequency dependent and, thus, the spatial interactions (which are not present in the one-dimensional model) must play a decisive role. Even if both objections are based on the errant mental image of the one-dimensional substitute system as a sort of spatial cross section of the three-dimensional topography, they illustrate the difficulty of accepting the method of reduction of dimensionality. The possibility of an equivalent replacement of a three-dimensional contact

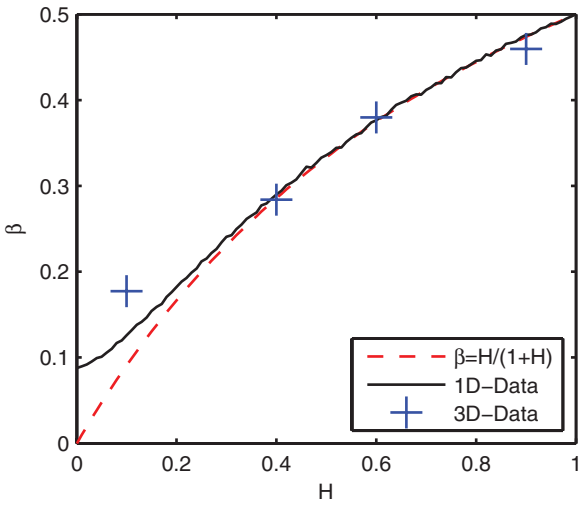

FIG. 4. (Color online) The dependency of the exponent β on the Hurst exponent H according to Eq. (5) (red broken line), estimated by one-dimensional indentations (black solid line), and by three-dimensional indentations (blue marks).

problem by that of one dimension seems at first glance miraculous, even if it was rigorously proven for elastic contacts of at least two classes of surface topographies, both regular and randomly rough. Though the validity of the method of reduction of dimensionality to viscoelastic bodies follows formally from Radok's theorems, a direct comparison with results of three-dimensional simulations could contribute to better understanding of the applicability area of the method. Therefore, in the present paper, the applicability of the method of reduction of dimensionality is proved by comparison with direct three-dimensional simulations of a contact between a linearly viscous elastomer and a rigid indenter having a fractal rough surface.

Within the method of reduction of dimensionality, the viscous media is described as a row of independent linear dashpots with a small spacing Δx each having the damping constant $\Delta d = 4\eta\Delta x$ [14]. For randomly rough surfaces, it was initially proposed in [14,23] that the surface of the indenter has to be transformed into a rigid line with the one-dimensional spectral density

$$C_{1D}(q) = \pi q C_{2D}(q). \tag{13}$$

In [13], it was shown, that a correction factor depending on the Hurst exponent has to be introduced to get the exact correspondence. The correct transformation has the form $C_{1D}(q) = \lambda(H)qC_{2D}(q)$, where $\lambda(H)$ is a constant which depends only on the Hurst exponent [31].

For illustrating the quality of the simulations with the method of reduction of dimensionality, we present the dependence of the power β in the dependency (9) in Fig. 4, which was calculated from three-dimensional simulations, one-dimensional simulations with the method of reduction of dimensionality, and according to the analytic approximation (5). Results obtained with the method of reduction of dimensionality are plotted as a solid black line. This curve represents the evaluation of the exponent β for 101 different Hurst exponents within the interval [0; 1], each averaged over 500 indentations with randomly generated one-dimensional "surfaces" with a size of 4,000,000 elements. Comparable results by means of boundary element calculations are marked by blue crosses. They are evaluated for four different Hurst exponents only. Each mark represents the average over about 250 indentations (a subset of the indentations represented in Fig. 2) with randomly generated surfaces consisting of 51 432 elements as shown in Fig. 1. The huge differences in the quantities of elements and evaluations are due to the high computational costs of the boundary element calculations in comparison to the one-dimensional calculations. The broken red line corresponds to the analytical equation (10). One can see that the power β calculated both with the exact three-dimensional simulation and with the one-dimensional reduction method nearly coincide with each other over the entirety of the interval of the studied Hurst exponents, and they are accurately described with the analytical equation (5), at least for $H > 0.4$.

The huge advantage of the reduction method over boundary element calculations is the demand of computation time. While the boundary element simulations presented in the figures require several weeks, the corresponding simulations by means of the reduction method were obtained in a few minutes.

VI. CONCLUSION

In conclusion, the indentation of a rigid body with a fractal, self-affine surface into a linearly viscous elastomer can be described by a power law. This is confirmed both by analytical arguments and numerical simulations. Further, we have proven the applicability of the method of reduction of dimensionality to a contact with a linearly viscous elastomer in a broad range of fractal dimensions of the roughness.

ACKNOWLEDGMENTS

The authors gratefully acknowledge useful discussions with A. Filippov and R. Pohrt. We acknowledge the financial support of the German Research Society (DFG).

[1] A. Khademhosseini, R. Langer, J. Borenstein, and J. P. Vacanti, Proc. Natl. Acad. Sci. USA **103**, 2480 (2006).
[2] K. R. Shull, Mater. Sci. Eng., R **36**, 1 (2002).
[3] A. Dawson, M. Rides, C. R. G. Allen, and J. M. Urquhart, Polym. Test. **27**, 555 (2008).
[4] B. N. J. Persson, J. Chem. Phys. **115**, 3840 (2001).
[5] F. P. Bowden and D. Tabor, *The Friction and Lubrication of Solids* (Clarendon Press, Oxford, 1986).
[6] J. F. Archard, Proc. R. Soc. London, Ser. A **243**, 190 (1957).
[7] J. A. Greenwood and J. B. P. Williamson, Proc. R. Soc. London, Ser. A **295**, 300 (1966).
[8] C. Campana and M. H. Müser, Phys. Rev. B **74**, 075420 (2006).

[9] S. Hyun and M. O. Robbins, Tribol. Int. **40**, 1413 (2007).
[10] S. Akarapu, T. Sharp, and M. O. Robbins, Phys. Rev. Lett. **106**, 204301 (2011).
[11] C. Campana, B. N. J. Persson, and M. H. Müser, J. Phys.: Condens. Matter **23**, 085001 (2011).
[12] R. Pohrt and V. L. Popov, Phys. Rev. Lett. **108**, 104301 (2012).
[13] R. Pohrt, V. L. Popov, and A. E. Filippov, Phys. Rev. E **86**, 026710 (2012).
[14] V. L. Popov, *Contact Mechanics and Friction. Physical Principles and Applications* (Springer, Berlin, 2010), p. 362.
[15] E. H. Lee, Quart. Appl. Math. **13**, 183 (1955).
[16] J. R. M. Radok, Quart. Appl. Math. **15**, 198 (1957).
[17] E. H. Lee and J. R. M. Radok, J. Appl. Mech. **27**, 438 (1960).
[18] T. C. T. Ting, J. Appl. Mech. **33**, 845 (1966).
[19] G. A. C. Graham, Int. J. Eng. Sci. **5**, 495 (1967).
[20] J. A. Greenwood, Int. J. Mech. Sci. **52**, 829 (2010).
[21] M. Vandamme and F. J. Ulm, Int. J. Solids Struct. **43**, 3142 (2006).
[22] F. Kozhevnikov, J. Cesbron, D. Duhamel, H. P. Yin, and F. Anfosso-Ledee, Int. J. Mech. Sci. **50**, 1194 (2008).
[23] T. Geike and V. L. Popov, Phys. Rev. E **76**, 036710 (2007).
[24] M. Heß, *Über die Abbildung ausgewählter dreidimensionaler Kontakte auf Systeme mit niedrigerer räumlicher Dimension* (Cuvillier-Verlag, Göttingen, 2011).
[25] M. Heß, Phys. Mesomech. **15**, 264 (2012).
[26] B. N. J. Persson, O. Albohr, U. Tartaglino, A. I. Volokitin, and E. Tosatti, J. Phys.: Condens. Matter **17**, R1 (2005).
[27] V. L. Popov, Phys. Mesomech. **15**, 254 (2012).
[28] S. Kürschner and A. E. Filippov, Phys. Mesomech. **15**, 270 (2012).
[29] V. L. Popov and S. G. Psakhie, Tribol. Int. **40**, 916 (2007).
[30] T. Geike and V. L. Popov, Tribol. Int. **40**, 924 (2007).
[31] V. L. Popov, Friction **1**, 41 (2013).